

Development of a flow rate monitoring method for the wearable ventricular assist device driver

Kentaro Ohnuma · Akihiko Homma · Hirohito Sumikura · Tomonori Tsukiya · Yoshiaki Takewa · Toshihide Mizuno · Hiroshi Mukaibayashi · Koichi Kojima · Kazuo Katano · Yoshiyuki Taenaka · Eisuke Tatsumi

Received: 9 July 2014 / Accepted: 5 December 2014 / Published online: 13 December 2014
© The Japanese Society for Artificial Organs 2014

Abstract Our research institute has been working on the development of a compact wearable drive unit for an extracorporeal ventricular assist device (VAD) with a pneumatically driven pump. A method for checking the pump blood flow on the side of the drive unit without modifying the existing blood pump and impairing the portability of it will be useful. In this study, to calculate the pump flow rate indirectly from measuring the flow rate of the driving air of the VAD air chamber, we conducted experiments using a mock circuit to investigate the correlation between the air flow rate and the pump flow rate as well as its accuracy and error factors. The pump flow rate was measured using an ultrasonic flow meter at the inflow and outflow tube, and the air flow was measured using a thermal mass flow meter at the driveline. Similarity in the instantaneous waveform was confirmed between the air flow rate in the driveline and the pump flow rate. Some limitations of this technique were indicated by consideration of the error factors. A significant correlation was found between the average pump flow rate in the ejecting direction and the average air flow rate in the ejecting direction ($R^2 = 0.704\text{--}0.856$), and the air flow rate in the filling direction ($R^2 = 0.947\text{--}0.971$). It was demonstrated

that the average pump flow rate was estimated exactly in a wide range of drive conditions using the air flow of the filling phase.

Keywords Flow rate monitoring · Wearable pneumatic drive unit · Ventricular assist devices (VADs) · Air mass flow

Introduction

Mechanical circulatory support using ventricular assist devices (VADs) has become a major option in the treatment of severe heart failure. Early VADs were used mainly as a bridge to heart transplantation (BTT). For BTT patients to be discharged and stay at home, the blood pump needs to be implanted; therefore, a wide variety of implantable devices have been developed [1, 2]. Annually, more than 1,000 patients are implanted with the current devices that use compact rotary pumps [2–4]. An overwhelming shortage of donor organs, however, is still a serious problem globally. Organ transplantation from brain-death donors was approved in 1997 in Japan [5], but the accumulative number of heart transplantations as of December 2013 was only 186.

Before two types of implantable VADs were approved in Japan in 2010 [6], the extracorporeal VAD with a pneumatically driven pump, originally developed at the National Cerebral and Cardiovascular Center, was the only VAD available in Japan (currently available as Nipro VAD, Nipro, Osaka, Japan) [7–11]. More than 900 patients have been treated with Nipro VAD, and about 50 patients are almost always being treated with this system in Japan [12]. The Nipro VAD has played an important role as a chronic-use device for patients, who are outside the

K. Ohnuma (✉) · H. Sumikura · T. Tsukiya · Y. Takewa · T. Mizuno · Y. Taenaka · E. Tatsumi
Department of Artificial Organs, National Cerebral and Cardiovascular Center Research Institute, 5-7-1 Fujishirodai, Suita-shi, Osaka 565-8565, Japan
e-mail: ohnuma.kentaro@ri.ncvc.go.jp

A. Homma · K. Katano
School of Science and Engineering, Tokyo Denki University, Saitama, Japan

H. Mukaibayashi · K. Kojima
IWAKI Co., Ltd., Saitama, Japan

application range of transplantation or not suitable for implantable VAD due to small body size, or as a temporary support for a bridge to decision [2, 6] in the acute severe heart failure patients.

The conventional driver of this pneumatic VAD is equipped with an air compressor, vacuum pump, and batteries. These components, however, make the driver heavy and bulky, which restricts the activity of the patients. Downsizing of the pneumatic VAD driver is one of the key factors for improving the patient's QOL by expanding the range of actions. The authors developed a portable driver for the Nipro VAD, the Mobart-NCVC driver (Senko Medical Instrument Manufacturing Co., Ltd.), which allows transportation in the hospital by the patient himself, and also enables long-distance transportation of patients from one institute to another for heart transplantation. The Mobart-NCVC uses an electro-hydraulic actuator and weighs 13 kg [13].

Our research institute has been working on the development of a more compact VAD driver consisting of a cylinder-piston actuator [14]. The current model of this driver, including its two batteries, weighs only 4.7 kg. The pump can be operated with the two batteries for more than 5 h under normal operating conditions. We are planning to add an additional flow meter to this driver, which will be useful to optimize the operating conditions of the VAD. A mass flow meter, which is capable of measuring the instantaneous flow rates of the driving air in the VAD air chamber, has been employed to calculate blood flow through the VAD. The present study introduces the air flow meter for our portable VAD driver and examines accuracy and errors of it in relation to the pump flow through experiments using a mock circuit. Correction methods for obtaining blood flow rates from the air flow rates are also investigated.

Materials and methods

Description of Nipro VAD blood pump

The Nipro VAD blood pump is a pneumatically driven diaphragm pump, as shown in Fig. 1b. The blood pump is mainly made from polyurethane resin (TM3) and consists of two mechanical heart valves. The priming volume of the blood pump is 70 mL, and is capable of generating 50–60 mL of blood flow per beat.

Wearable pneumatic drive unit (WPD)

The structure of the mechanism in the WPD for generating air pressure is depicted in Fig. 1. Air pressure to drive the diaphragm of the blood pump is generated by converting

the rotation of the brushless DC motor into linear motion via a crankshaft directly connected to the cylinder piston. The internal capacity of this cylinder piston is 109 mL. Two regulating valves at the air outlets adjust the driving positive or negative pressure by releasing or drawing the air from or into the tube. The ratio of systole duration (SD) is predetermined by the built-in noncircular gears [14]. The current model of the WPD is also equipped with a pressure release valve at the bottom dead center to compensate for any change in the amount of air in the air circuit due to air leaks from pressure control or changes in room air conditions. The top dead center and bottom dead center of the cylinder piston can be detected with built-in proximity sensors. The experiments in the present study were conducted using three drive units with SD ratios of 35, 40, and 45 % (WPD100-SD35, SD40, and SD45).

Measurement of air flow rates

Figure 2 shows the experimental setup. The Nipro VAD blood pump was connected to an overflow-type mock circuit (IWAKI Co., Ltd.). The working fluid was tap water at 25 °C. The WPD was connected to the Nipro VAD via a 1.35-m air driveline. The air flow rates in the driveline were measured using a thermal gas mass flow meter (model 4043, TSI Inc.), which was installed in the driveline 750 mm away from the blood pump. This mass flow meter possesses a good accuracy (up to 2 % or 0.05 L/min) and response (4 ms) with low resistance. The measurement of the reverse flow with this flow meter has the uncertainty of 2.5 % of the reading in comparison with it of the flow of the forward direction. The forward direction of the flow meter was set as the ejecting direction of VAD. The flow rates of the blood pump were measured using ultrasonic flow meters (T106, Transonic Systems Inc.) installed in the tubes on the inflow and outflow sides of the pump. The air pressures of the WPD were measured using piezoelectric pressure transducers (PA-500, Nidec Copal Electronics Corp.). The position of the cylinder piston was detected from the pulse signals at the top dead center and bottom dead center of the cylinder piston. The flow meter was able to output the volumetric flow rates under a standard condition (at 21.11 °C and 101.3 kPa). Because the pressure in the driveline widely varied during pump operation, flow rates were corrected using the following equation:

$$Q_{aVF} = Q_{aStdF} \left[\frac{273.15 + T}{273.15 + 21.11} \right] \left[\frac{759.8}{759.8 + P} \right] \quad (1)$$

where Q_{aVF} is the converted volumetric flow rate of the air driveline, Q_{aStdF} is the reading from the flow meter, P is the pressure of the driveline, and T is temperature of the air (°C). T was approximately assumed room temperature because it was difficult to exactly measure the

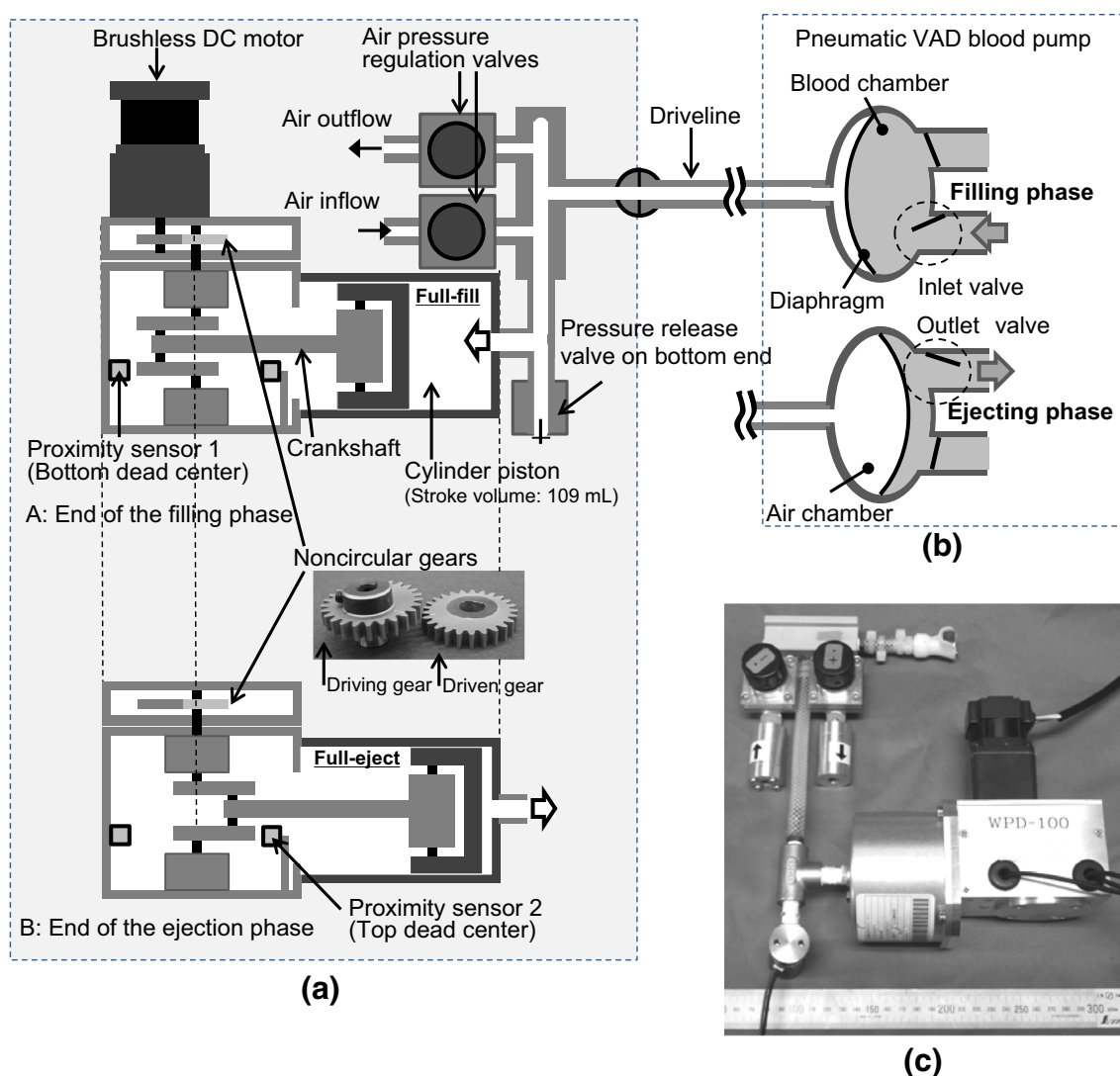


Fig. 1 Overview of the WPD-100 drive unit. **a** WPD-100 mechanism for generating air pressure. **b** Mechanism for generating pulsatile flow on the pneumatic blood pump. **c** Photograph of the core unit, air regulation valves and pressure release valves

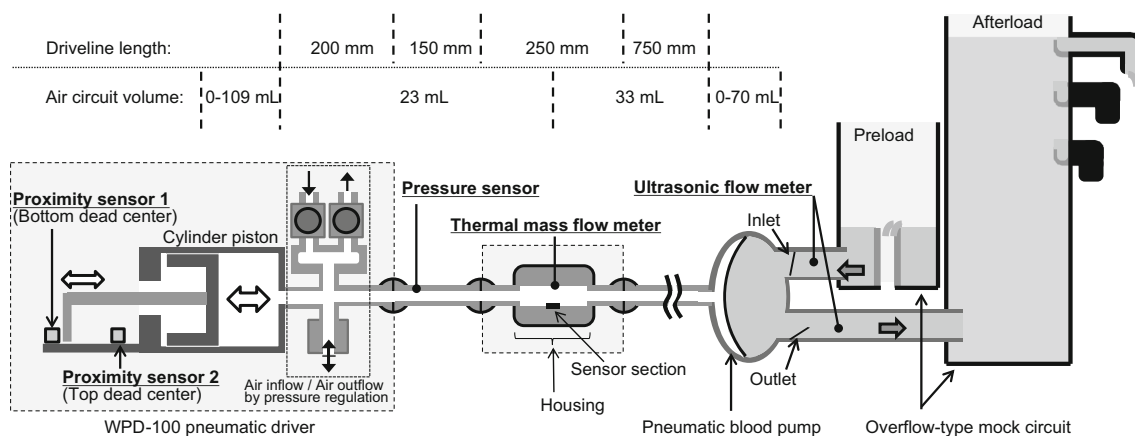


Fig. 2 Schematic diagram of equipment composition and the experimental circuit (air circuit of the pneumatic driver side and mock circuit of the pump output side)

instantaneous value of air temperature in the driveline with high responsiveness.

Test conditions

The preload to the blood pump was kept constant at 10 mmHg using the overflow-type mock circuit, and the afterload was set to 80, 100, and 120 mmHg, respectively. The measurements were conducted with SD ratios of 35, 40, and 45 % using the three types of drive units, and beating rates of 60, 70, 80, 90, and 100 bpm. The pressure of the blood pump was adjusted using the air pressure regulation valves of the drive unit so that almost full filling and full ejection driving was achieved by visual inspection.

Results

Figure 3 shows an example waveform when the blood pump was driven by WPD100-SD40 at 70 bpm, with an afterload of 100 mmHg and a preload of 10 mmHg. The output from the air flow meter demonstrated sufficient response to the ejection and the filling of the VAD. The output of the air flow meter, $Q_{a \text{ StdF}}$, during the filling phase was positive in Fig. 3b because all the air flow passed through the sensor is output as a signal of positive direction, and does not indicate the direction of the air flow. Based on the signal of the proximity sensors of the WPD, we were able to easily divide the waveform into the ejecting phase and the filling phase and to change the waveform direction of the filling phase into the real flow direction as shown in Fig. 3d.

Reflux components generated by the mechanical valve that are not reflected in the air flow rate and flow components for a period during which the inflow and outflow of the pump occur simultaneously were detected (Fig. 3c). Similar trends were also obtained under other driving conditions (Fig. 4a, b). The average of the reflux components shown in Fig. 4a was 0.69 ± 0.077 L/min. Ratios of the flow component shown in Fig. 4b to the pump flow rate were a maximum of 3.9 % (SD 35 %, HR: 100 bpm, afterload: 80 mmHg) and a minimum of 1.3 % (SD 45 %, HR: 60 bpm, afterload: 120 mmHg) under all test conditions.

Figure 3d shows a comparison between the converted air flow rates, $Q_{a \text{ VF}}$, and the blood flow rates, Q_p . During ejection, phase deviation between the air and blood was observed due to compressibility. The deviation is illustrated as the shadowed area between the waveforms of the air flow rate and the blood flow rate in Fig. 3d. The Nipro VAD employs active filling via the negative pressure generated by the vacuum pump in the console, but the deviation was found to be smaller during the filling phase.

Similar trends were also obtained under other driving conditions. Except for this deviation, there is sufficient similarity of the outputs from the air flow meter to those from the blood flow meter.

As one example, the significant deviations during the ejecting phase at SD40 are shown in Fig. 4c as the capacity in one cycle under each driving condition. The capacity of the air circuit in the latter part of the air flow meter was approximately 103 mL at the end of the pump ejection phase and approximately 33 mL at the end of the filling phase. As shown in Fig. 4c, the capacity required for compression to raise the pressure of the air of this capacity from 0 to 250 mmHg (approximate value of the maximum driving pressure) was calculated as 18.9 mL from the capacity of the air circuit at the end of the ejection phase and as 6.1 mL from the capacity at the end to the filling phase, using formulae of changes in gas state (2) and (3), where polytropic index, n was set to 1.4.

$$PV^n = \text{const.} \quad (2)$$

$$\frac{V_1}{V_2} = \left(\frac{P_2}{P_1} \right)^{\frac{1}{n}} \quad (3)$$

The average flow rates were obtained by integrating the flow rate waveforms obtained for the ejecting and filling periods. The correlations of the pump outlet flow rate during the ejecting phase and the air flow rates during the ejecting phase are shown in Fig. 5a, and the pump outlet flow rate during the ejecting phase and the air flow rates during the filling phase are shown in Fig. 5b. Good linearity was found in the average air flow rates in the filling directions (in the forward direction, SD45: $R^2 = 0.781$, SD40: $R^2 = 0.704$, SD35: $R^2 = 0.856$; and in the backward direction, SD45: $R^2 = 0.969$, SD40: $R^2 = 0.947$, SD35: $R^2 = 0.971$). However, deviations from the blood flow meter were found both in the ejecting and filling directions. The average flow rate measured by the air flow meter was approximately 90 % lower than that measured by the blood flow meter in the forward direction and approximately 120 % higher in the backward direction.

Discussion

In this study, similarity in the instantaneous waveform was confirmed between the air flow rate in the driveline and the pump flow rate. A significant correlation was particularly recognized between the average blood flow rates and the air flow rates of the filling direction. On the other hand, some limitations of this technique were suggested by the deviation between the air flow and blood flow observed due to compressibility of the air and the error factors that were not reflected in the air flow, as described below.

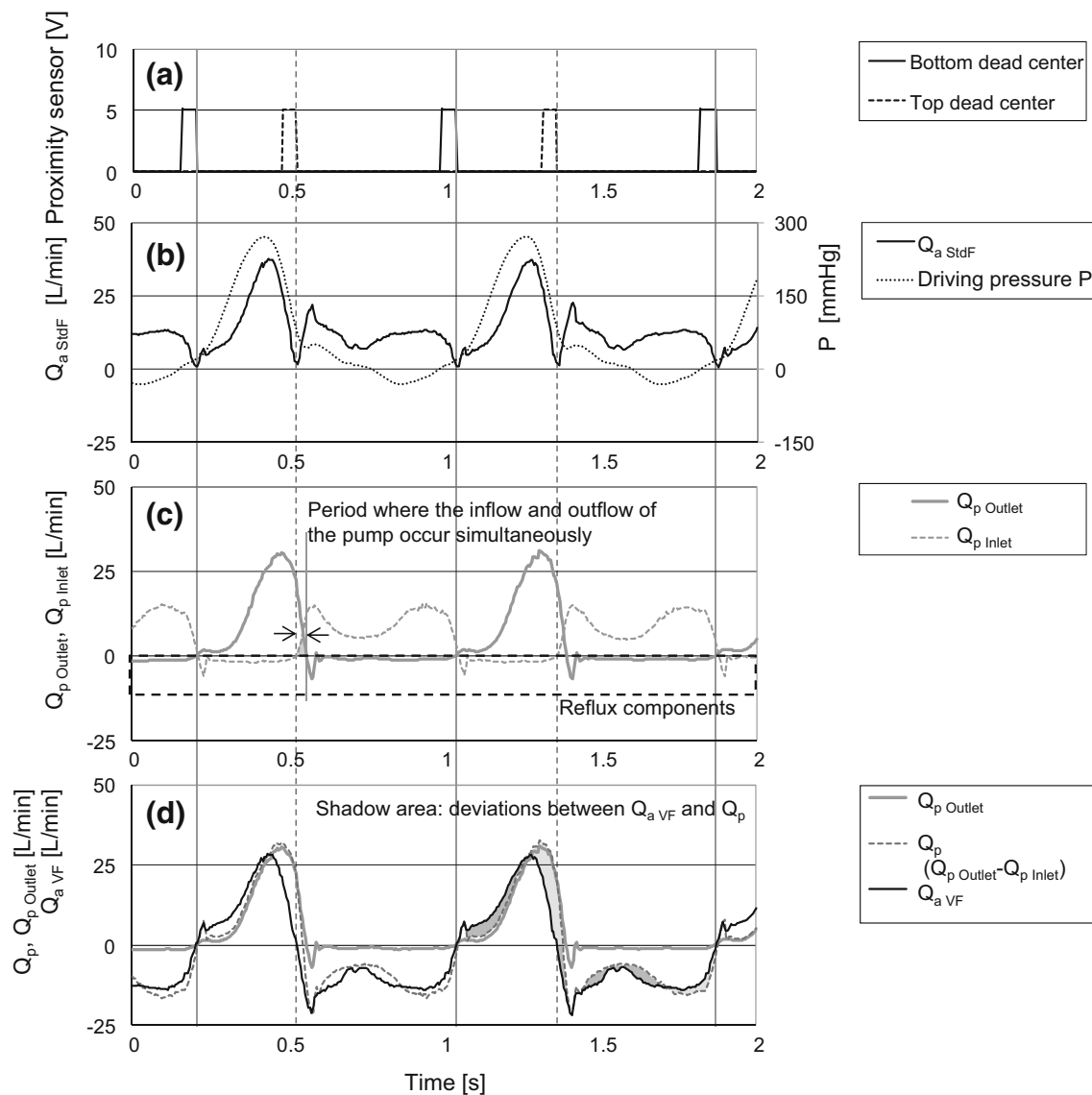


Fig. 3 Example of instantaneous waveforms when the blood pump was driven by WPD100-SD40 at 70 bpm, with an afterload of 100 mmHg. **a** Positions of the cylinder piston detected with proximity sensors, **b** measured air flow and driving pressure, **c** pump flow rate

measured at the inlet and outlet sides of the pump, **d** converted volumetric flow rate of the air driveline, $Q_{a \text{ VF}}$, and the flow rates into and out of the blood chamber of the pump, Q_p

Error factors that were not reflected in the air flow

Deviations between the air flow and blood flow could be attributed to several causes. For instance, there may be components that flow due to inertia during the period where the inflow and outflow of the pump occur simultaneously, as shown in Figs. 3c and 4b. This phenomenon is remarkable, especially at higher beating rates. The effect of this flow is not reflected in the air flow because it does not cause any volumetric changes in the blood pump chamber. However, any flow rate not generated by movement of the diaphragm has the range from 1.3 to 3.9 % under any test condition, so it was considered that these flow rates

negligibly influence the estimation of flow rate. Similarly, reflux components generated by the mechanical valve are not reflected in the air flow rate (Figs. 3c, 4a). However, it was considered from Fig. 4a that the reflux components could be corrected using a constant term in the estimate of the pump flow rate.

The point that the room temperature was used when converting the volumetric air flow rate can be cited as another error factor. The air temperature in the driveline measured with the temperature sensor to be built into the air flow meter was up to 38 °C under all test conditions (response time of the sensor: 75 ms, room temperature: 25 °C). Compared with the volumetric air flow converted

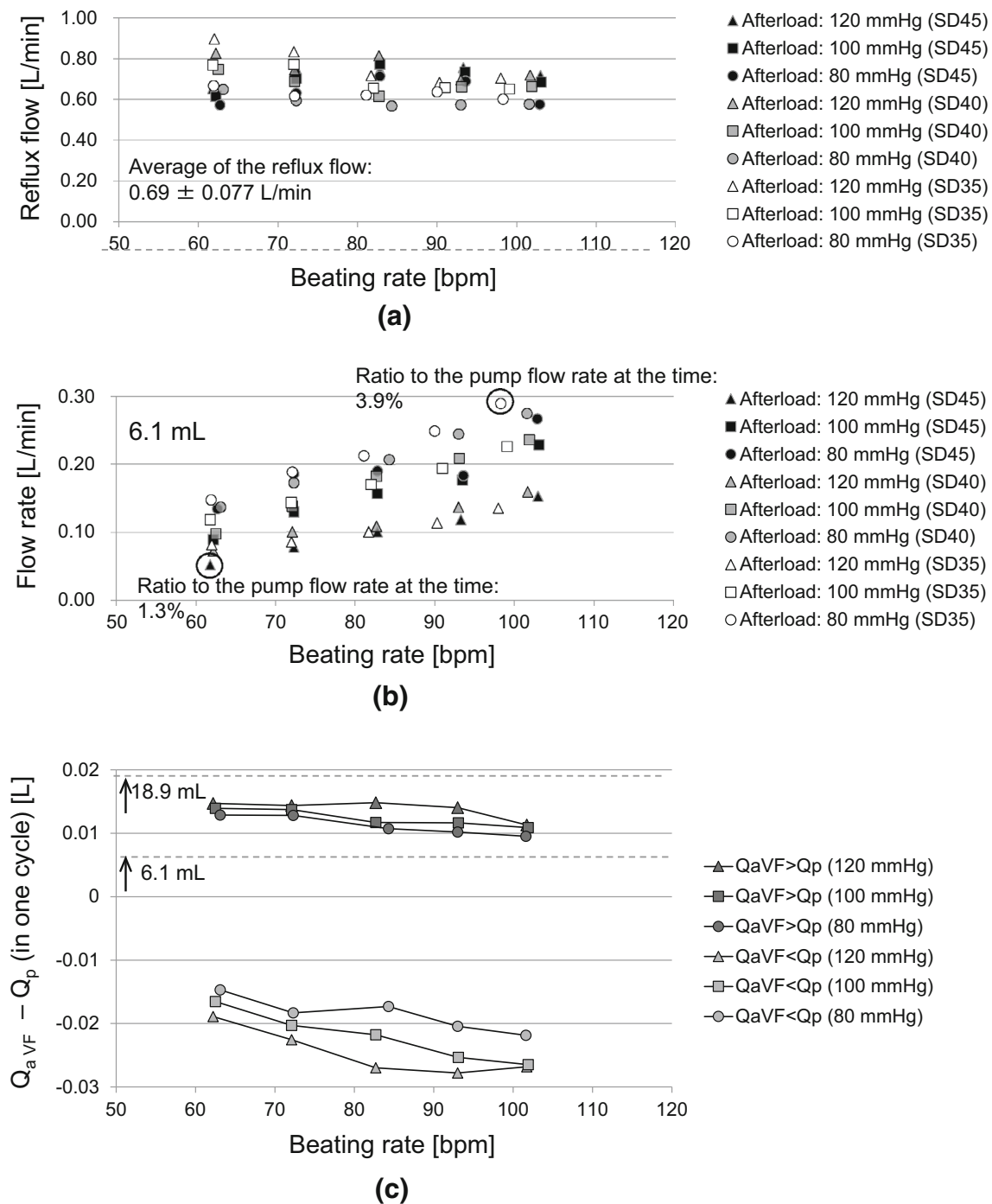


Fig. 4 Deviations between the air flow and blood flow. **a** Reflux components generated by the mechanical. **b** Flow components for a period during which the inflow and outflow of the pump occur

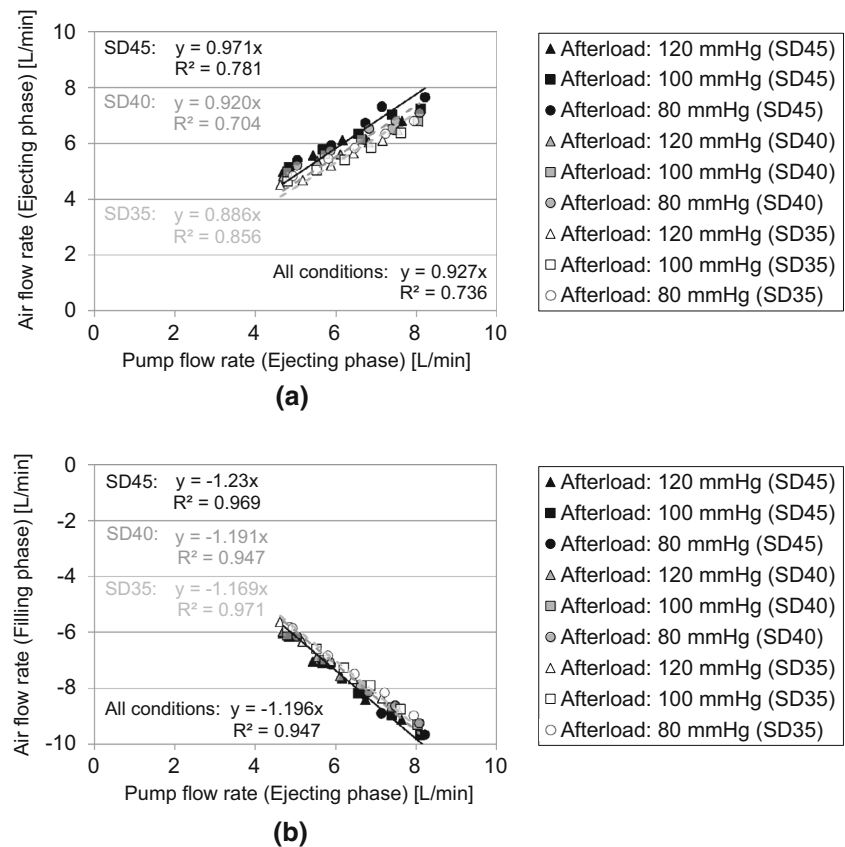
simultaneously. **c** Example of differences between Q_{aVF} and Q_p during one cycle with WPD-100 SD40

with room temperature, the air flow converted with the air temperature in the driveline is increased up to 4.3 % from Eq. (1). The influence of the temperature is considered to be limited, the use of a higher responsive temperature sensor, however, will be able to contribute to improve the accuracy of the measurement of the volumetric air flow.

Deviation due to compressibility of the air

As shown in Fig. 3d, the deviation between the air flow rates and blood flow rates is apparently larger during the ejecting phase than during the filling phase. From the results shown in Figs. 3d and 4c, the capacity difference in

Fig. 5 Correlation between the average pump flow rate in the ejecting direction and the average air flow rate. **a** The air flow rates during the ejecting phase. **b** The air flow rates during the filling phase



the initial stage of ejection was found to be within the range of 6.1–18.9 mL. The deviation in the initial stage of ejection was considered to be mainly caused by the compression process of the air.

During the latter half of the ejection phase, the fluid flow on the blood chamber side of the pump generated by volumetric expansion of the air while releasing the driving pressure in the air chamber of the pump to push out the diaphragm after passing through the sensor section of the air flow meter (an element that is hardly reflected in the air flow meter) was considered to be the main factor causing the deviation.

During the filling phase, on the other hand, the magnitude of the negative pressure is relatively low, and the difference in the flow rate was smaller than that during the ejection phase.

Linearity of the average flow rate

As shown in Fig. 5a, b, the linearity of the average flow rate was higher in the air flow rate of the filling direction than that of the ejecting direction, because of the deviation with compressibility of the air during the ejecting phase and the volumetric air flow conversion with room temperature. The deviations from the blood flow meter were slightly low for

the air flow rate of the ejecting direction. The estimation error of the average blood flow likely decreases under a wide range of driving conditions because of the high linearity when the air flow rate in the filling direction is used. Furthermore, estimation of the pump flow rate is considered stable and fully possible using our method because of high correlation with the pump flow and the air flow.

Practical application and availability

In the present study, the conversion from the standard air flow rate to the volumetric flow rate and the calculation of the average flow rate were performed offline. For practical applications, the estimate of the pump flow rate should be automatically calculated in real time, using the air flow of the filling direction. This is feasible using a general microprocessor because of the simple algorithm using the proximity sensors of the WPD and the linearity between the pump flow rate and the air flow rate. The air flow meter was installed in the driveline in this experiment. The flow meter should be installed into the WPD system not to impair the portability of the WPD. This problem was considered to be solved using a small embedded flow sensor.

It is possible, of course, to measure the blood flow rate in a pneumatic VAD using an ultrasonic flow meter, but the

flow meter needs to be built into the system for a patient to be able to carry it around. It is necessary for the probe to be attached to the outflow tube crossing the skin. To date, various, indirect methods for measuring the blood flow rate in a pneumatic blood pump (or the internal capacity of the pump) have been attempted. While techniques that use electric impedance, capacitance, or ultrasonic waves [15–18] are useful for measuring the pump capacity in real time, these techniques require sensors or electrodes to be attached at positions near the blood chamber of the pump housing. Our method of measuring pump blood flow at the side of the drive unit from the air flow without modifying the existing blood pump may have disadvantage for the accuracy and the measurement of the instantaneous value because of estimating the pump flow rate indirectly. It, however, has an advantage of not disturbing the care of sites that the inflow and outflow conduits cross the skin. In addition, it has a sufficient measurement performance of the average pump flow rate.

Conclusion

A flow measurement method for the portable driver of a pneumatically driven VAD using an air flow meter for estimating the pump flow has been investigated. Limitations of this technique were indicated by the deviation between the air flow and blood flow resulting from compressibility of the air and the blood flow components that were not reflected in the air flow. A significant correlation was particularly recognized between the average blood flow rates and the air flow rates of the filling direction. It was demonstrated that the average pump flow rate was estimated exactly in a wide range of drive conditions using the air flow of the filling phase. This technique is useful for monitoring the pump blood flow in the case when a pneumatic VAD is driven by a WPD.

Acknowledgments This study was supported in part by Grant-in-Aid for Scientific Research (B) (No. 24390308) and Grant-in-Aid for Challenging Exploratory Research (No. 25670563) from the Japan Society for the Promotion of Science and the Ministry of Education, Culture, Sports, Science and Technology of Japan.

Conflict of interest The authors declare that they have no conflict of interest.

References

1. Stewart GC, Givertz MM. Mechanical circulatory support for advanced heart failure: patients and technology in evolution. *Circulation*. 2012;125(10):1304–15.
2. Slaughter MS, Pagani FD, Rogers JG, Miller LW, Sun B, Russell SD, Starling RC, Chen L, Boyle AJ, Chillcott S, Adamson RM, Blood MS, Camacho MT, Idrissi KA, Petty M, Sobieski M, Wright S, Myers TJ, Farrar DJ. Clinical management of continuous-flow left ventricular assist devices in advanced heart failure. *J Heart Lung Transplant*. 2010;29(45):S1–39.
3. Kirklin JK, Naftel DC, Kormos RL, Stevenson LW, Pagani FD, Miller MA, Baldwin JT, Young JB. The fourth INTERMACS annual report: 4,000 implants and counting. *J Heart Lung Transplant*. 2012;31(2):117–26.
4. Kirklin JK, Naftel DC, Kormos RL, Stevenson LW, Pagani FD, Miller MA, Baldwin JT, Young JB. Fifth INTERMACS annual report: risk factor analysis from more than 6,000 mechanical circulatory support patients. *J Heart Lung Transplant*. 2013;32(2):141–56.
5. Ishii M, Hamamoto M. Bioethics and organ transplantation in Japan. *JMAJ*. 2009;52(5):289–92.
6. Kyo S, Minami T, Nishimura T, Gojo S, Ono M. New era for therapeutic strategy for heart failure: destination therapy by left ventricular assist device. *J Cardiol*. 2012;59(2):101–9.
7. Shiga T, Kinugawa K, Hatano M, Yao A, Nishimura T, Endo M, Kato N, Hirata Y, Kyo S, Ono M, Nagai R. Age and preoperative total bilirubin level can stratify prognosis after extracorporeal pulsatile left ventricular assist device implantation. *Circ J*. 2011;75(1):121–8.
8. Takano H, Taenaka Y, Noda H, Kinoshita M, Yagura A, Tatsumi E, Sekii H, Umezu M, Nakatani T. Multi-institutional studies of the national cardiovascular center ventricular assist system: use in 92 patients. *ASAIO Trans*. 1989;35:541–4.
9. Takano H, Nakatani T, Taenaka Y. Clinical experience with ventricular assist systems in Japan. *Ann Thorac Surg*. 1993;55:250–5.
10. Saito S, Matsumiya G, Sakaguchi T, Fujita T, Kuratani T, Ichikawa H, Sawa Y. Fifteen-year experience with Toyobo paracorporeal left ventricular assist system. *J Artif Organs*. 2009;12:27–34.
11. Takatani S, Matsuda H, Hanatani A, Nojiri C, Yamazaki K, Motomura T, Ohuchi K, Sakamoto T, Yamane T. Mechanical circulatory support devices (MCS) in Japan: current status and future directions. *J Artif Organs*. 2005;8:13–27.
12. Japanese Association for Clinical Ventricular Assist Systems. Japanese Registry for ventricular assist device. 2013. http://www.jacvas.com/VAS_registry2012.pdf. Accessed 28 May 2014. (in Japanese).
13. Nishinaka T, Taenaka Y, Tatsumi E, Ohnishi H, Homma A, Shioya K, Mizuno T, Tsukiya T, Mushika S, Hashiguchi Y, Suzuki A, Kitamura S. Development of a compact portable driver for a pneumatic ventricular assist device. *J Artif Organs*. 2007;10:236–9.
14. Homma A, Taenaka Y, Tatsumi E, Akagawa E, Lee H, Nishinaka T, Takewa Y, Mizuno T, Tsukiya T, Kakuta Y, Katagiri N, Shimosaki I, Hamada S, Mukaibayashi H, Iwaoka W. Development of a compact wearable pneumatic drive unit for a ventricular assist device. *J Artif Organs*. 2008;11:182–90.
15. Gawlikowski M, Darlak M, Pustelny T, Kustosz R. Preliminary investigations regarding the possibility of acoustic resonant application for blood volume measurement in pneumatic ventricular assist device. *Mol Quantum Acoust*. 2006;27:89–96.
16. Gawlikowski M, Pustelny T, Kustosz R, Darlak M. Non invasive blood volume measurement in pneumatic ventricular assist device POLVAD. *Mol Quantum Acoust*. 2006;27:97–106.
17. Kamimura T, Homma A, Tsukiya T, Kakuta Y, Lee H, Tatsumi E, Taenaka Y, Kitamura S. Monitoring of diaphragm position in pulsatile pneumatic ventricular assisted device by ultrasound sensor (a new method for flow measurement in VAD). *JSME Int J Ser C*. 2004;47:1124–7.
18. Sasaki E, Nakatani T, Taenaka Y, Takano H, Hirose H. Novel method to determine instantaneous blood volume in pulsatile blood pump using electrical impedance. *Artif Organs*. 1994;18:603–10.